SIAM J. IMAGING SCIENCES
Vol. 7, No. 1, pp. 456–475

A New Convex Optimization Model for Multiplicative Noise and Blur Removal*

Xi-Le Zhao†, Fan Wang‡, and Michael K. Ng§

Abstract. The main contribution of this paper is to propose a new convex optimization model for multiplicative noise and blur removal. The main idea is to rewrite a blur and multiplicative noise equation such that both the image variable and the noise variable are decoupled. The resulting objective function involves the total variation regularization term, the term of variance of the inverse of noise, the ℓ_1-norm of the data-fitting term among the observed image, and noise and image variables. Such a convex minimization model can be solved efficiently by using many numerical methods in the literature. Numerical examples are presented to demonstrate the effectiveness of the proposed model. Experimental results show that the proposed model can handle blur and multiplicative noise (Gamma, Gaussian, or Rayleigh distribution) removal quite well.

Key words. convex optimization, image restoration, multiplicative noise, total variation, alternating direction method

AMS subject classifications. 65F22, 68U10, 35A15, 65K10, 52A41

DOI. 10.1137/13092472X

1. Introduction.

Image deblurring and denoising are important problems in signal and image processing. Usually, imaging systems capture an image $\mathbf{f}$ and generate a degraded image $\mathbf{g}$. A common model of the degradation process is given by

$$\mathbf{g} = \mathbf{H}\mathbf{f} + \mathbf{n}, \tag{1.1}$$

where an original image $\mathbf{f} \in \mathbb{R}^m$ is corrupted by a spatial-invariant blur matrix $\mathbf{H} \in \mathbb{R}^{m\times m}$ and a noise vector $\mathbf{n} \in \mathbb{R}^m$, and the observed image is $\mathbf{g} \in \mathbb{R}^m$. We remark in image restoration that $\mathbf{H}$ is usually a matrix of block Toeplitz with Toeplitz blocks (BTTB) when zero boundary conditions are applied, and block Toeplitz-plus-Hankel with Toeplitz-plus-Hankel blocks (BTHTHB) when Neumann boundary conditions are used [24]. The recovery of $\mathbf{f}$ from $\mathbf{g}$ is an ill-posed inverse problem. The regularization method based on total variation (TV) [29]

*Received by the editors June 12, 2013; accepted for publication (in revised form) November 19, 2013; published electronically March 4, 2014.
http://www.siam.org/journals/siims/7-1/92472.html
†School of Mathematical Sciences, University of Electronic Science and Technology of China, Chengdu 611731, People's Republic of China, and Centre for Mathematical Imaging and Vision, Hong Kong Baptist University, Kowloon Tong, Hong Kong (xlzhao.122003@163.com). This author's research was supported by 973 Program (2013CB329404), NSFC (61170311, 61370147), Chinese Universities Specialized Research Fund for the Doctoral Program (20110185110020), Sichuan Province Sci. and Tech. Research Project (2012GZX0080), and the Fundamental Research Funds for the Central Universities (ZYGX2013J106).
‡School of Mathematics and Statistics, Lanzhou University, Lanzhou 730000, People's Republic of China (wangfan2009@lzu.edu.cn). This author's research was supported by NSFC (11301239) and the Fundamental Research Funds for the Central Universities (lzujbky-2013-12).
§Corresponding author. Centre for Mathematical Imaging and Vision, and Department of Mathematics, Hong Kong Baptist University, Kowloon Tong, Hong Kong (mng@math.hkbu.edu.hk). This author's research was supported by RGC GRF grant 202013 and HKBU FRG grant FRG/12-13/065.

has been shown to be successful for this image restoration problem because of its ability to preserve sharp discontinuities (edges) in restored images.

In (1.1), the additive noise assumption is made. In recent years, many researchers have studied the multiplicative noise assumption; see [2, 20, 22, 28, 31]. The model of the degradation process is given by

$$\mathbf{g} = \mathbf{Hf} \circ \mathbf{n}, \tag{1.2}$$

where $\circ$ refers to the componentwise multiplication. One can see that when $H = I$, the degradation process reduces to the multiplicative noise degradation. There are many applications for multiplicative noise removal, for example, magnetic field inhomogeneity in magnetic resonance imaging (MRI) [13, 23], speckle noise in ultrasound [37], and speckle noise in synthetic aperture radar (SAR) images [2, 36]. In these applications, $\mathbf{n}$ is assumed to follow some probability distributions. For instance, the Gamma distribution is considered in SAR [2, 36], and the Rayleigh distribution is studied in ultrasound imaging [37]. On the other hand, the degradation by blur and multiplicative noise occurs in many optical coherent imaging systems [39]. In some imaging systems, nonlinear image restoration problems [33] are required to be solved. One approach is to transform such nonlinear image restoration problems into the model in (1.2), where both blur and multiplicative noise appear.

1.1. Multiplicative noise removal. When $\mathbf{H}$ is the identity matrix, this refers to multiplicative noise removal only. In the literature, the first method is based on TV regularization by Rudin, Lions, and Osher [28] (RLO model). The discrete setting is given by

$$\min_{\mathbf{f}} \|\mathbf{Df}\|_2 \quad \text{subject to} \quad \sum_{i=1}^{m} \frac{[\mathbf{g}]_i}{[\mathbf{f}]_i} = 1 \quad \text{and} \quad \sum_{i=1}^{m} \left(\frac{[\mathbf{g}]_i}{[\mathbf{f}]_i} - 1 \right)^2 = \sigma^2, \tag{1.3}$$

where $\mathbf{D}$ is the first-order difference matrix with respect to the x- and y-directions of an image $\mathbf{f}$, and $\|\mathbf{Df}\|_2$ is just the TV regularization term. In (1.3), the mean of noise is assumed to be 1, and the variance of noise is equal to σ^2. Rudin, Lions, and Osher [28] designed a gradient-based projection algorithm to find the minimizer. The objective function is nonconvex and it is very expensive to solve for a global minimizer of (1.3).

The second method is given by Aubert and Aujol [2] (AA model):

$$\min_{\mathbf{f}} \sum_{i=1}^{m} \left(\log[\mathbf{f}]_i + \frac{[\mathbf{g}]_i}{[\mathbf{f}]_i} \right) + \lambda \|\mathbf{Df}\|_2. \tag{1.4}$$

The objective function is derived by using maximum a posteriori (MAP) estimation approach when a Gamma distribution is used for noise $\mathbf{n}$. Although the objective function is nonconvex, Aubert and Aujol showed the existence of minimizers of the objective function, gave a sufficient condition ensuring the uniqueness, and proved that a comparison principle holds. They also employed a gradient method to show the capability of their model on some numerical examples.

Recently, Shi and Osher [31] proposed considering a noisy observation given by $\log \mathbf{g} = \log \mathbf{f} + \log \mathbf{n}$, and derived the TV minimization model for multiplicative noise removal problems.

Huang, Ng, and Wen [20] used the transformation $\mathbf{f} = \exp \mathbf{z}$ in (1.4), and considered the TV regularization for $\mathbf{z}$ in the following model (EXP model):

$$\min_{\mathbf{f}} \sum_{i=1}^{m} ([\mathbf{z}]_i + [\mathbf{g}]_i \exp(-[\mathbf{z}]_i)) + \lambda \|\mathbf{D}\mathbf{z}\|_2. \tag{1.5}$$

The resulting objective function is strictly convex. They developed an alternating minimization algorithm to find the minimizer of such objective function efficiently and showed the convergence of the minimization method. Bioucas-Dias and Figueiredo [3] used a variable splitting and split-Bregman method to solve the minimization problem. We remark that the models in [3, 20, 31] are convex in $\mathbf{z}$ (i.e., in the logarithm domain) but are not convex in $\mathbf{f}$ in the original image domain. Also it is not straightforward to extend these methods to handle blur and noise removal by considering $\log(\mathbf{H}\mathbf{f})$ in the models.

Steidl and Teuber [32] studied the variational model consisting of the Kullback–Leibler (KL) divergence as the data-fitting term, and the TV or nonlocal means as the regularization term. In the continuous setting, the minimizer of the Shi–Osher model is the same as that of the KL divergence-TV multiplicative noise model. Teuber, Steidl, and Chan [35] further considered the KL divergence constrained minimization problem, where the model parameter can be estimated by some statistical methods where the knowledge of noise is available. Recently, Yun and Woo [40] proposed using the mth root transformation to deal with the nonconvexity of the AA model.

Durand, Fadili, and Nikolova [10] proposed a method composed of several stages. They also used the log-image data and applied a reasonable suboptimal hard thresholding on its curvelet transform; then they applied a variational method by minimizing a specialized hybrid criterion composed of an ℓ_1 data-fidelity term of the thresholded curvelet coefficients and a TV regularization term in the log-image domain. The restored image can be obtained by using an exponential of the minimizer, weighted in such a way that the mean of the original image is preserved. Their restored images combine the advantages of shrinkage and variational methods. Besides the above approaches, dictionary learning methods and nonlocal mean methods have also been proposed and developed for multiplicative noise removal, see [18, 34]. In particular, Teuber and Lang [34] considered nonlocal filters in a weighted maximum likelihood estimation framework where the weights are defined by a new similarity measure based on the analysis of a probabilistic measure for a noise model (see the work by Deledalle, Denis, and Tupin [8]).

1.2. Blur removal. There are some papers dealing with both blur and multiplicative noise removal; see [2, 3, 9, 28, 38]. Both the RLO and AA models can be extended to deal with blur removal:

$$\min_{\mathbf{f}} \|\mathbf{D}\mathbf{f}\|_2 \quad \text{subject to} \quad \sum_{i=1}^{m} \frac{[\mathbf{g}]_i}{[\mathbf{H}\mathbf{f}]_i} = 1 \quad \text{and} \quad \sum_{i=1}^{m} \left(\frac{[\mathbf{g}]_i}{[\mathbf{H}\mathbf{f}]_i} - 1 \right)^2 = \sigma^2 \tag{1.6}$$

and

$$\min_{\mathbf{f}} \sum_{i=1}^{m} \left(\log[\mathbf{H}\mathbf{f}]_i + \frac{[\mathbf{g}]_i}{[\mathbf{H}\mathbf{f}]_i} \right) + \lambda \|\mathbf{D}\mathbf{f}\|_2, \tag{1.7}$$

according to (1.3) and (1.4), respectively. These two objective functions are still nonconvex, and the computational costs of minimizing such objective functions are expensive via the gradient projection method [2, 28]. In [19], Huang, Zeng, and Ng considered a variational approach to handling the multiplicative noise removal and deblurring problem by adding a Gaussian noise term in the model. The approximation model is solved by an alternating minimization method. In [38], Wang and Ng studied a constrained TV-regularized image restoration model on log-image domain, approximated a set of nonconvex constraints by a set of convex constraints, and then applied the alternating direction method of multipliers to solve the resulting optimization problem. Recently, Dong and Zeng [9] proposed some convex relaxation models consisting of a MAP estimator based on Gamma noise, a quadratic term, and the TV regularization. The quadratic term is based on the statistical property of the Gamma noise. Under a mild condition, the uniqueness of the solution is guaranteed. We remark that the multiplicative noise is assumed to be a Gamma distribution in the above-mentioned methods [2, 9, 19, 38].

1.3. The contribution. The main contribution of this paper is to propose a new convex optimization model for multiplicative noise and blur removal. The main idea is to rewrite (1.2) as follows:

$$\mathbf{g} = \mathbf{NHf}, \tag{1.8}$$

where $\mathbf{N}$ is a diagonal matrix where the main diagonal entries of $\mathbf{N}$ are given by $[\mathbf{n}]_i$. Since $\mathbf{f}$ and $\mathbf{n}$ are coupled together in (1.2) or (1.8), it is clear that the optimization model involving both $\mathbf{f}$ and $\mathbf{n}$ (or the statistical derivation of a term for $\mathbf{n}$) would be nonconvex; see (1.6) or (1.7). According to (1.2), when there is no noise in the observed image, we can express $\mathbf{n} = \mathbf{e}$ (a vector of all ones), i.e., $\mathbf{n}$ is not a zero vector. When there is a multiplicative noise in the observed image, we expect that $[\mathbf{n}]_i \neq 1$, but it is greater than zero. Assume that $\mathbf{N}$ is invertible, we can further rewrite (1.8) into the following form:

$$\mathbf{Gw} = \mathbf{Hf}, \tag{1.9}$$

where $\mathbf{G}$ is a diagonal matrix where the main diagonal entries of $\mathbf{G}$ are given by $[\mathbf{g}]_i$, and $\mathbf{w}$ is a vector with $[\mathbf{w}]_i = 1/[\mathbf{n}]_i$. Now it is interesting to note in (1.9) that both $\mathbf{f}$ and $\mathbf{w}$ are decoupled, and a convex optimization model can be proposed and developed for multiplicative noise and blur removal based on (1.9).

The rest of this paper is organized as follows. In section 2, we develop the the new convex model, and present the numerical method for solving it. In section 3, experimental results are reported to demonstrate the effectiveness of the proposed model and the efficiency of the proposed numerical scheme. Finally, some concluding remarks are given in section 4.

2. The proposed model. In this paper, we propose the following convex optimization model for multiplicative noise and blur removal:

$$\min_{\mathbf{w},\mathbf{f}} \ \frac{1}{2}\|\mathbf{w} - \mu\mathbf{e}\|_2^2 + \alpha_1\|\mathbf{Gw} - \mathbf{Hf}\|_1 + \alpha_2\|\mathbf{Df}\|_2, \tag{2.1}$$

where α_1 and α_2 are two positive regularization parameters to control the balance among the three terms in the objective function, μ can be set to be the mean value of $\mathbf{w}$, and $\mathbf{e}$ is a vector

of all ones. One can see that if $H = I$, then the proposed model reduces to an unconditional convex model for multiplicative denoising. The first term in (2.1) is to measure the variance of $\mathbf{w}$, and therefore we would like to determine $\mathbf{w}$ and $\mathbf{f}$ in the model such that the variance of $\mathbf{w}$ can be minimized. The second term in (2.1) is the fitting term between the observed image, $\mathbf{f}$ and $\mathbf{w}$. Since $[\mathbf{w}]_i$ refers to the inverse of $[\mathbf{n}]_i$, the value of $[\mathbf{w}]_i$ may be very large. We employ the ℓ_1-norm to measure the fitting term so that a large value of $[\mathbf{Gw} - \mathbf{Hf}]_i$ can be ignored in the restoration process. The third term in (2.1) is the TV regularization of $\mathbf{f}$.

Theorem 2.1. *The model* (2.1) *is jointly convex for* $(\mathbf{f}, \mathbf{w})$.

Proof. Since a convex function with an affine mapping remains convex, the convex ℓ_1-norm with the affine mapping $(\mathbf{H}, -\mathbf{G})\begin{pmatrix}\mathbf{f}\\ \mathbf{w}\end{pmatrix}$ is jointly convex for $(\mathbf{f}, \mathbf{w})$. By combining the convexity of the quadratic norm and the TV regularization term, the objective function in (2.1) is jointly convex for $(\mathbf{f}, \mathbf{w})$. ∎

Now let us provide some remarks for the proposed model in (2.1) for multiplicative noise and blur removal.

1. The ℓ_1-norm is used in the data-fitting term instead of the ℓ_2-norm. Figure 1(a) shows an observed image of multiplicative Gamma noise of mean 1 and variance 0.1 without blur. In Figure 1(b), we show the restored image by using the ℓ_2-norm of the data-fitting term. We see that there are some pixel values of large magnitudes; see Figure 1(c). In Figure 1(d), we show the image by removing the pixel values of large magnitudes, and it is more clear compared with the picture in Figure 1(b). In order to remove pixel values of large magnitudes automatically, we can adapt the ℓ_1-norm of the data-fitting term directly in the objective function; see the restored image in Figure 1(e).

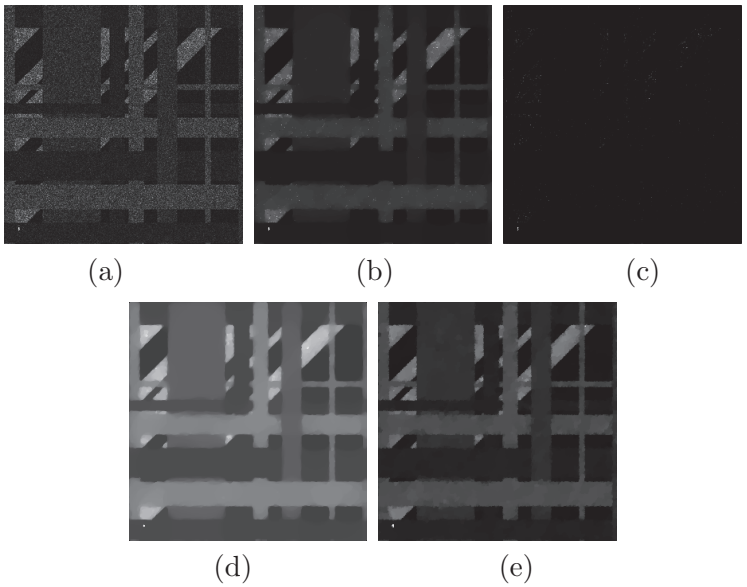

Figure 1. (a) *The observed image,* (b) *the restored image using the* ℓ_2*-norm of the data-fitting term,* (c) *the pixel values of large magnitudes,* (d) *the restored image after removing the pixel values of large magnitudes,* (e) *the restored image using the* ℓ_1*-norm of the data-fitting term.*

2. It would not be desirable to use only the data-fitting term $\|\mathbf{Gw} - \mathbf{Hf}\|_1$ and the TV regularization term $\|\mathbf{Df}\|_2$ in (2.1). In such a setting, $\mathbf{w}$ would be arbitrary. Indeed, if we minimize

$$\min_{\mathbf{w},\mathbf{f}} \ \|\mathbf{Gw} - \mathbf{Hf}\|_1 + \alpha\|\mathbf{Df}\|_2, \tag{2.2}$$

then $\mathbf{f} = \psi\mathbf{1}$ and $\mathbf{w} = \psi\mathbf{G}^{-1}\mathbf{H1}$ are trivial global minimizers of (2.2), and the corresponding objective function value is zero. We note that the variance term $\|\mathbf{w} - \mu\mathbf{e}\|_2^2$ is used to determine a better global minimizer by choosing the one with the minimal variance of $\mathbf{w}$ with respect to μ.

3. As the proposed model involves the minimization of the variance of the inverse of noise, we need to input the mean of the inverse of noise so that we can compute the variance term in the objective function. Here we demonstrate that when we have the mean and variance of n, the mean of the inverse of n can be estimated. Let us consider the Gamma, Rayleigh, and Gaussian noises.

The Gamma noise. The probability density function of Gamma noise n is given by

$$p(n) = \frac{n^{k-1}}{\Gamma(k)\theta^k} \exp\left(\frac{-n}{\theta}\right), \tag{2.3}$$

with $\theta > 0$ and $k > 1$. The mean value of n is equal to $k\theta$, and the variance of n is equal to $k\theta^2$. According to (2.3), we can derive that the mean value of $1/n$ is equal to

$$\begin{aligned}
\mathbb{E}(1/n) &= \frac{\Gamma(k-2)}{\theta^2\Gamma(k)} \int_0^{+\infty} n \frac{n^{k-3}}{\Gamma(k-2)\theta^{k-2}} \exp\left(-\frac{n}{\theta}\right) dn \\
&= \frac{\Gamma(k-2)}{\theta^2\Gamma(k)} \theta(k-2) \\
&= \frac{\theta(k-2)}{\theta^2(k-1)(k-2)} \\
&= \frac{1}{\theta(k-1)} \qquad (2.4)
\end{aligned}$$

when $k > 1$. In some cases, we set the mean value of Gamma noise to be 1 and use only one parameter L to express the noise level. More precisely, we set $k = L$ and $\theta = 1/L$. When L is small, the noise level is higher. It follows that $\mathbb{E}(1/n)$ is equal to $L/(L-1)$.

The Rayleigh noise. The probability density function of Rayleigh noise n is given by

$$p(n) = \frac{n}{\sigma^2} \exp\left(-\frac{n^2}{2\sigma^2}\right),$$

where σ is a positive parameter. The mean value of n is equal to $\sqrt{\pi/2}\sigma$, and the variance of n is equal to $(2 - \pi/2)\sigma^2$. We can derive a closed form formula for the mean value of the

inverse of Rayleigh noise as follows:

$$\begin{aligned}\mathbb{E}(1/n) &= \int_0^{+\infty} \frac{1}{n}\frac{n}{\sigma^2}\exp\left(-\frac{n^2}{2\sigma^2}\right) dn \\ &= \frac{\sqrt{2}}{\sigma}\int_0^{+\infty} \exp\left(-\left(\frac{n}{\sqrt{2}\sigma}\right)^2\right) d\frac{n}{\sqrt{2}\sigma} \\ &= \sqrt{\frac{\pi}{2\sigma^2}}. \end{aligned} \tag{2.5}$$

The Gaussian noise. However, for other probability density functions of multiplicative noises, it may be difficult to have a closed form solution for the mean value of $1/n$. For example, the probability density function of Gaussian noise n is given by

$$p(n) = \frac{1}{\sigma\sqrt{2\pi}}\exp\left(-\frac{(n-\mu)^2}{2\sigma^2}\right),$$

where the mean value of n is equal to μ, and the variance of n is equal to σ^2. We cannot derive a closed form formula for the mean value of the inverse of Gaussian noise. The mean value of the inverse of Gaussian noise is given by

$$\int_{-\infty}^{+\infty} \frac{1}{n}\frac{1}{\sigma\sqrt{2\pi}}\exp\left(-\frac{(n-\mu)^2}{2\sigma^2}\right) dn. \tag{2.6}$$

The above integral can be numerically approximated using high-order global adaptive quadratures (e.g., the adaptive Gauss–Kronrod quadrature [30]) to obtain an approximate value of the mean of the inverse of noise.

Assuming the noise is in a multiplicative form, there are quite a few methods which are able to provide enough accurate estimations of the expected value and the standard variance [1, 12, 27]. However, the detailed discussion of estimation methods is beyond the scope of this paper.

2.1. The numerical method. As the proposed model is a convex optimization problem, there are efficient solvers for finding a global minimizer of (2.1). The solvers include the Bregman method [15], proximal splitting methods [6] and primal-dual methods [5, 11], Douglas–Rachford methods [7], and alternating direction method of multipliers [14]. Here we just discuss the alternating direction method of multipliers. The other methods can also be applied and implemented.

We begin by reformulating (2.1) as the following constrained optimization problem:

$$\min_{\mathbf{w},\mathbf{f}} \frac{1}{2}\|\mathbf{w} - \mu\mathbf{e}\|_2^2 + \alpha_1\|\mathbf{z}\|_1 + \alpha_2\|\mathbf{p}\|_2$$

subject to $\mathbf{p} = \mathbf{D}\mathbf{f}$, $\mathbf{s} = \mathbf{G}\mathbf{w}$, and $\mathbf{z} = \mathbf{H}\mathbf{f} - \mathbf{s}$. The resulting augmented Lagrangian function

is given by

$$
\begin{aligned}
L(\mathbf{f},\mathbf{s},\mathbf{p},\mathbf{z},\mathbf{w},\lambda) &= \frac{1}{2}\|\mathbf{w}-\mu\mathbf{e}\|_2^2+\alpha_1\|\mathbf{z}\|_1+\alpha_2\|\mathbf{p}\|_2 \\
&\quad+\left\langle\begin{pmatrix}\lambda_1\\ \lambda_2\\ \lambda_3\end{pmatrix},\begin{pmatrix}\mathbf{D}&\mathbf{0}\\ \mathbf{H}&-\mathbf{I}\\ \mathbf{0}&\mathbf{I}\end{pmatrix}\begin{pmatrix}\mathbf{f}\\ \mathbf{s}\end{pmatrix}+\begin{pmatrix}-\mathbf{I}&\mathbf{0}&\mathbf{0}\\ \mathbf{0}&-\mathbf{I}&\mathbf{0}\\ \mathbf{0}&\mathbf{0}&-\mathbf{G}\end{pmatrix}\begin{pmatrix}\mathbf{p}\\ \mathbf{z}\\ \mathbf{w}\end{pmatrix}\right\rangle \\
&\quad+\beta\left\|\begin{pmatrix}\mathbf{D}&\mathbf{0}\\ \mathbf{H}&-\mathbf{I}\\ \mathbf{0}&\mathbf{I}\end{pmatrix}\begin{pmatrix}\mathbf{f}\\ \mathbf{s}\end{pmatrix}+\begin{pmatrix}-\mathbf{I}&\mathbf{0}&\mathbf{0}\\ \mathbf{0}&-\mathbf{I}&\mathbf{0}\\ \mathbf{0}&\mathbf{0}&-\mathbf{G}\end{pmatrix}\begin{pmatrix}\mathbf{p}\\ \mathbf{z}\\ \mathbf{w}\end{pmatrix}\right\|_2^2, \qquad (2.7)
\end{aligned}
$$

where λ_1, λ_2, and λ_3 are the vectors corresponding to the Lagrange multipliers to the linear constraints, and β is the penalty parameter of the alternating direction method of multipliers to control the speed of the convergence; see, for instance, [25]. The optimization problem is well structured since all the variables are separated into two groups, $(\mathbf{f},\mathbf{s})$ and $(\mathbf{p},\mathbf{z},\mathbf{w})$. This allows us to solve them more easily on their corresponding subproblems in the alternating direction method of multipliers.

In step 1, we solve for the variables $\mathbf{p}$, $\mathbf{z}$, and $\mathbf{w}$ in the subproblem. Since the variables $\mathbf{p}$, $\mathbf{z}$, and $\mathbf{w}$ are decoupled, their optimal solutions can be calculated separately as follows:

$$
[\mathbf{p}]_i^{k+1}=\max\left\{\left\|[\mathbf{D}\mathbf{f}^k+\frac{\lambda_1^k}{\beta}]_i\right\|_2-\frac{\alpha_2}{\beta},0\right\}\frac{\left(\mathbf{D}\mathbf{f}^k+\frac{\lambda_1^k}{\beta}\right)_i}{\left\|\left(\mathbf{D}\mathbf{f}^k+\frac{\lambda_1^k}{\beta}\right)_i\right\|_2},\quad i=1,\dots,m, \qquad (2.8)
$$

where $[\mathbf{p}]_i^{k+1}\in\mathbb{R}^2$ and $0\cdot(0/0)=0$ is assumed;

$$
[\mathbf{z}]_i^{k+1}=\max\left\{\left|\left[\mathbf{H}\mathbf{f}^k-\mathbf{s}^k+\frac{\lambda_2^k}{\beta}\right]_i\right|-\frac{\alpha_1}{\beta},0\right\}\circ\ \operatorname{sign}\left[\mathbf{H}\mathbf{f}^k-\mathbf{s}^k+\frac{\lambda_2^k}{\beta}\right]_i,\quad i=1,\dots,m, \qquad (2.9)
$$

where sign refers to 1 if the entry is greater than or equal to zero, and -1 if the entry is negative; and

$$
[\mathbf{w}]_i^{k+1}=\frac{[\mu e+\beta\mathbf{G}\mathbf{s}^k+\mathbf{G}\lambda_3^k]_i}{[I+\beta\mathbf{G}^T\mathbf{G}]_{i,i}},\quad i=1,\dots,m, \qquad (2.10)
$$

where $\mathbf{G}^T$ denotes the transpose of $\mathbf{G}$, and the superscript k of each variable refers to the iterate at the kth iteration of the alternating direction method of multipliers. We note that $[I+\beta\mathbf{G}^T\mathbf{G}]_{i,i}$ is always greater than zero. The computational complexities of updating the variables $\mathbf{p}$, $\mathbf{z}$, and $\mathbf{w}$ in (2.8), (2.9), and (2.10) are $O(m)$, $O(m\log m)$, and $O(m)$ operations, respectively.

In step 2, we solve for the variables $\mathbf{f}$ and $\mathbf{s}$ in the subproblem. The subproblem is a least squares problem given by

$$
\left\|\begin{pmatrix}\mathbf{D}&\mathbf{0}\\ \mathbf{H}&-\mathbf{I}\\ \mathbf{0}&\mathbf{I}\end{pmatrix}\begin{pmatrix}\mathbf{f}\\ \mathbf{s}\end{pmatrix}-\begin{pmatrix}\mathbf{p}^k-\frac{\lambda_1^k}{\beta}\\ \mathbf{z}^k-\frac{\lambda_2^k}{\beta}\\ \mathbf{G}\mathbf{w}^k-\frac{\lambda_3^k}{\beta}\end{pmatrix}\right\|_2^2, \qquad (2.11)
$$

and the corresponding solution can be obtained by solving the normal equation as follows:

$$\begin{pmatrix} \mathbf{D}^T\mathbf{D}+\mathbf{H}^T\mathbf{H} & -\mathbf{H}^T \\ -\mathbf{H} & 2\mathbf{I} \end{pmatrix}\begin{pmatrix} \mathbf{f} \\ \mathbf{s} \end{pmatrix} = \begin{pmatrix} \mathbf{D}^T\left(\mathbf{p}^k-\frac{\lambda_1^k}{\beta}\right)+\mathbf{H}^T\left(\mathbf{z}^k-\frac{\lambda_2^k}{\beta}\right) \\ -\left(\mathbf{z}^k-\frac{\lambda_2^k}{\beta}\right)+\left(\mathbf{G}\mathbf{w}^k-\frac{\lambda_3^k}{\beta}\right) \end{pmatrix}. \tag{2.12}$$

When $\mathbf{H}$ is a blurring matrix generated by a symmetric point spread function, $\mathbf{H}$ can be diagonalized by a fast transform matrix $\mathbf{\Phi}$, i.e., $\mathbf{H} = \mathbf{\Phi}^T\mathbf{\Lambda}_1\mathbf{\Phi}$ [16]. As $\mathbf{D}$ is a first-order difference matrix, $\mathbf{D}^T\mathbf{D}$ can also be diagonalized by the same transform matrix $\mathbf{\Phi}$, i.e., $\mathbf{D}^T\mathbf{D} = \mathbf{\Phi}^T\mathbf{\Lambda}_2\mathbf{\Phi}$. For a detailed discussion, we refer the reader to [16, 24]. Therefore we obtain the following decomposition:

$$\begin{pmatrix} \mathbf{D}^T\mathbf{D}+\mathbf{H}^T\mathbf{H} & -\mathbf{H}^T \\ -\mathbf{H} & 2\mathbf{I} \end{pmatrix} = \begin{pmatrix} \mathbf{\Phi}^T & \mathbf{0} \\ \mathbf{0} & \mathbf{\Phi}^T \end{pmatrix}\begin{pmatrix} \mathbf{\Lambda}_1^T\mathbf{\Lambda}_1+\mathbf{\Lambda_2}^T\mathbf{\Lambda}_2 & -\mathbf{\Lambda}_1^T \\ -\mathbf{\Lambda}_1 & 2\mathbf{I} \end{pmatrix}\begin{pmatrix} \mathbf{\Phi} & \mathbf{0} \\ \mathbf{0} & \mathbf{\Phi} \end{pmatrix},$$

and the normal equations can be solved by using fast transforms in $O(m \log m)$ operations.

In step 3, we update the Lagrange multipliers λ_1, λ_2, and λ_3 as follows:

$$\begin{pmatrix} \lambda_1^{k+1} \\ \lambda_2^{k+1} \\ \lambda_3^{k+1} \end{pmatrix} = \begin{pmatrix} \lambda_1^{k} \\ \lambda_2^{k} \\ \lambda_3^{k} \end{pmatrix} + \beta\left[\begin{pmatrix} \mathbf{D} & \mathbf{0} \\ \mathbf{H} & -\mathbf{I} \\ \mathbf{0} & \mathbf{I} \end{pmatrix}\begin{pmatrix} \mathbf{f}^{k+1} \\ \mathbf{s}^{k+1} \end{pmatrix} + \begin{pmatrix} -\mathbf{I} & \mathbf{0} & \mathbf{0} \\ \mathbf{0} & -\mathbf{I} & \mathbf{0} \\ \mathbf{0} & \mathbf{0} & -\mathbf{G} \end{pmatrix}\begin{pmatrix} \mathbf{p}^{k+1} \\ \mathbf{z}^{k+1} \\ \mathbf{w}^{k+1} \end{pmatrix}\right].$$

The alternating direction method of multipliers iterates steps 1, 2, and 3 until the convergence. The total cost of each iteration is $(m \log m)$ operations. Also the convergence of the method for the above convex objective function is guaranteed. In the next section, we present some numerical results to show the effectiveness of the proposed model.

3. Numerical experiments. In this section, we report numerical results on the image restoration for blurred images corrupted by multiplicative noise. The results of the proposed convex model (CONVEX) are compared with those of the AA model by Aubert and Aujol [2] and the EXP model by Bioucas-Dias and Figueiredo [3]. The AA model is solved by the gradient method. The EXP model is also solved by the alternating direction method of multipliers. In our implementation, we use one more splitting variable to solve the associated TV subproblem exactly. In [3], the Chambolle iterative method is employed to solve the associated subproblem. The stopping criteria of all numerical methods are measured on the relative change of the successive iterates ($\mathbf{f}_k$ and $\mathbf{f}_{k-1}$) being less than a specified tolerance: $\|\mathbf{f}_k - \mathbf{f}_{k-1}\|_2/\|\mathbf{f}_{k-1}\|_2 \le 5 \times 10^{-4}$. The initial guess is set to be the observed image unless otherwise specified. All the tests are performed under Windows 7 and MATLAB Version 7.10 (R2010a) running on a desktop with an Intel Core2 Quad CPU at 2.66 GHz with 4 GB of memory.

The testing images are given in Figure 2. The quality of the restored images is measured by the highest peak signal-to-noise ratio (PSNR) which is defined as follows:

$$\mathrm{PSNR} = 10\log_{10}\frac{\max_i\{[\mathbf{f}]_i, [\tilde{\mathbf{f}}]_i\}}{\frac{1}{m}\sum_{i=1}^m([\mathbf{f}]_i - [\tilde{\mathbf{f}}]_i)^2},$$

(a) (b)

Figure 2. *The original images* (a) *Cameraman and* (b) *Parrot.*

Table 1
The denoising results of different models.

Images	Noise	AA model			EXP model			CONVEX model		
		PSNR	Iter	Time	PSNR	Iter	Time	PSNR	Iter	Time
(a)	Gaussian	26.34	2771.0	26.0	25.83	177.0	6.0	26.86	300.0	9.0
	Gamma	24.00	3473.0	37.0	24.16	216.0	8.0	24.39	410.0	14.0
	Rayleigh	21.75	3424.0	34.0	21.54	313.0	12.0	21.94	87.0	3.0
(b)	Gaussian	25.56	1510.0	16.0	25.70	177.0	8.0	27.21	290.0	10.0
	Gamma	21.63	2416.0	25.0	23.79	216.0	10.0	24.75	331.0	11.0
	Rayleigh	20.59	3907.0	40.0	20.62	301.0	14.0	20.74	86.0	3.0

where $\mathbf{f}$ and $\tilde{\mathbf{f}}$ are the original image and the restored image, respectively.

Our empirical evidences indicate that the ratio α_1/α_2 is almost a constant which depends on the type of noise for the case of denoising or the type of blur for the case of deblurring. In the denoising scenario, we find that the ratios are 1.4, 1.2, and 1.6 for Gaussian noise, Gamma noise, and Rayleigh noise, respectively. In the deblurring scenario, we find that the ratios are 2.1, 2.3, and 1.2 for motion blur, Gaussian blur, and Moffat blur, respectively. Based on this observation, we can tune the parameter α_2 according to the noise level of the inverse noise w and set the other parameter α_1 according to the corresponding ratio. For the other methods (the AA model [2] and the EXP model [3]), we choose the corresponding regularization parameter such that the PSNR result is highest.

3.1. Image denoising. In the first experiment, we test the performance of our CONVEX method of three types of multiplicative noise (Gaussian, Gamma, and Rayleigh). The Gaussian noise is generated by the MATLAB built-in function "randn". The Gamma noise is generated by the MATLAB built-in function "gamrnd". The Rayleigh noise is generated by $\sigma\sqrt{-2\log(1-u)}$, where u is a uniformly distributed random variable generated by the MATLAB built-in function "rand"; see [21]. The means of the Gaussian, Gamma, and Rayleigh noises are set to be 1, and the variances of the Gaussian, Gamma, and Rayleigh noises are 0.04, 0.1, and 0.2728, respectively. Here we set the values of μ based on the formulas in (2.4), (2.5), and (2.6) in the proposed model. In Table 1, we show the PSNR values, iterations, and computational time (in seconds) of the restored images by different methods. We note that each entry of the table refers to a number by taking the average results of ten noise cases under the same experimental setting (type of noise and level of noise). Here the iteration number is rounded up to the integer, and computational time is rounded up to the second. The values

(a) (b) (c) (d)

Figure 3. (a) *The observed image corrupted by the Gaussian noise, and the restored image by* (b) *the AA model* ($\alpha = 2 \times 10^{-1}$), (c) *the EXP model* ($\alpha = 6 \times 10^{-1}$), *and* (d) *the CONVEX model* ($\alpha_2 = 8 \times 10^{-4}$).

(a) (b) (c) (d)

Figure 4. (a) *The observed image corrupted by the Gamma noise, and the restored image by* (b) *the AA model* ($\alpha = 3 \times 10^{-1}$), (c) *the EXP model* ($\alpha = 8 \times 10^{-1}$), *and* (d) *the CONVEX model* ($\alpha_2 = 9 \times 10^{-4}$).

(a) (b) (c) (d)

Figure 5. (a) *The observed image corrupted by the Rayleigh noise, and the restored image by* (b) *the AA model* ($\alpha = 6 \times 10^{-1}$), (c) *the EXP model* ($\alpha = 1.4 \times 10^{0}$), *and* (d) *the CONVEX model* ($\alpha_2 = 7 \times 10^{-3}$).

of the corresponding regularization parameters can be found in the captions of Figures 3–8. We see that the proposed model performs quite well in terms of PSNR values and iterations. The values of used regularization parameters of different methods are shown in Figures 3–8. In Figures 3–8, we further display the denoised images by using different models. It is clear from the figures that the restoration results of the CONVEX model are visually better than those of the AA and EXP methods.

3.2. Image deblurring. In the second experiment, we test the performance of our CONVEX method for image deblurring. We test three kinds of blurs, namely motion blur, Gaussian blur, and Moffat blur. Their MATLAB commands are fspecial('motion',5,30), fspe-

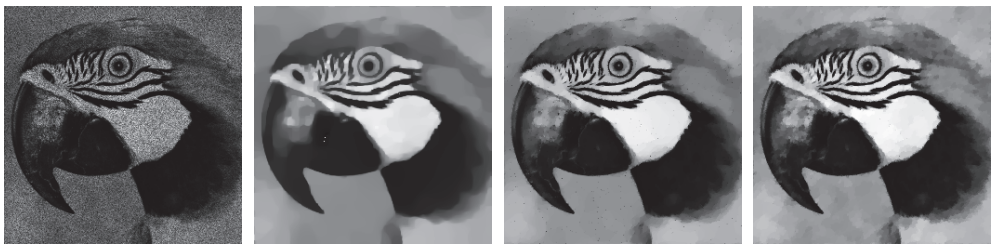

(a) (b) (c) (d)

Figure 6. (a) *The observed image corrupted by the Gaussian noise, and the restored image by* (b) *the AA model* ($\alpha = 4 \times 10^{-1}$), (c) *the EXP model* ($\alpha = 6 \times 10^{-1}$), *and* (d) *the CONVEX model* ($\alpha_2 = 8 \times 10^{-4}$).

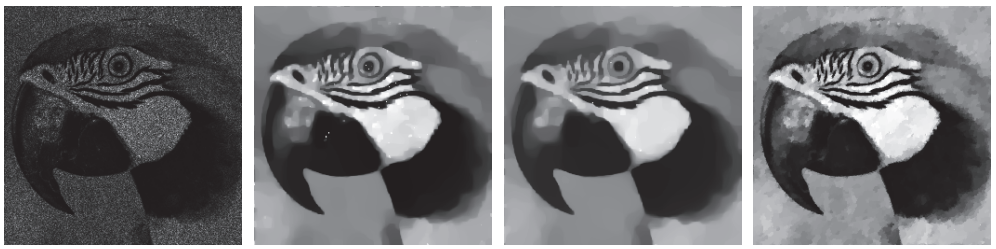

(a) (b) (c) (d)

Figure 7. (a) *The observed image corrupted by the Gamma noise, and the restored image by* (b) *the AA model* ($\alpha = 5 \times 10^{-1}$), (c) *the EXP model* ($\alpha = 8 \times 10^{-1}$), *and* (d) *the CONVEX model* ($\alpha_2 = 8 \times 10^{-4}$).

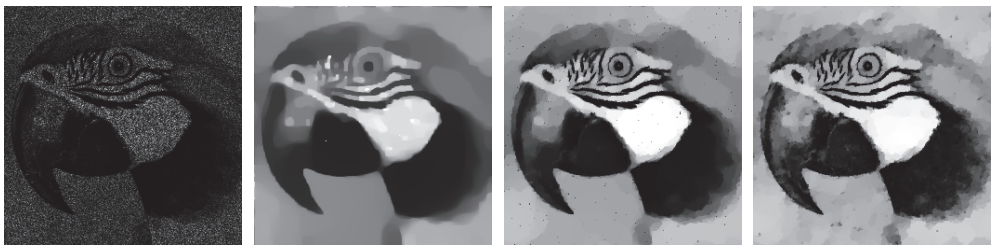

(a) (b) (c) (d)

Figure 8. (a) *The observed image corrupted by the Rayleigh noise, and the restored image by* (b) *the AA model* ($\alpha = 6 \times 10^{-1}$), (c) *the EXP model* ($\alpha = 1.4 \times 10^{0}$), *and* (d) *the CONVEX model* ($\alpha_2 = 6 \times 10^{-3}$).

cial('gaussian',[7,7],2), and psfMoffat([7,7],1,5), which is a function in the HNO package.[1] The blurred images are contaminated by multiplicative Gamma noise with mean 1 and $L = 10$. As the AA model is nonconvex, we also test two different initial guesses including the observed image $\mathbf{g}$ (guess 1) and the perturbed version of observed images $\mathbf{g}$+20∗rand(m,m) (guess 2). Here we set the values of μ based on (2.4) in the proposed model. In Table 2, we show the PSNR values, iterations, and computational time of the restored images by different methods. Each entry of the table refers to a number resulting from taking the average results of ten noise cases under the same experimental setting (type of blur and level of noise). Here the iteration

[1]The HNO package is available at http://www2.imm.dtu.dk/~pch/HNO/.

Table 2
The deblurring results by different models.

Images	Blurs	AA model (guess 1)			AA model (guess 2)			CONVEX model		
		PSNR	Iter	Time	PSNR	Iter	Time	PSNR	Iter	Time
(a)	Motion	22.17	3247.0	80.0	21.32	3262.0	83.0	23.35	93.0	4.0
	Gaussian	21.32	3168.0	78.0	20.61	3173.0	77.0	22.42	35.0	2.0
	Moffat	23.82	3465.0	83.0	22.64	3475.0	82.0	24.10	52.0	2.0
(b)	Motion	21.80	3344.0	81.0	20.99	3358.0	82.0	23.18	106.0	5.0
	Gaussian	20.31	3190.0	73.0	19.71	3198.0	73.0	21.33	25.0	1.0
	Moffat	23.04	2585.0	67.0	21.88	3207.0	83.0	24.42	73.0	3.0

number is rounded up to the integer, and computational time is rounded up to the second. The values of the corresponding regularization parameters can be found in the captions of Figures 9–14. We see that the proposed model performs quite well in terms of PSNR values, iterations, and computational time (in seconds). The values of regularization parameters used by the different methods are shown in Figures 9–14. In Figures 9–14, we display the restored images by using different models. It is clear from the figures that the restoration results of the CONVEX model are visually better than those of the AA method. In the tables and figures, the AA model is sensitive to the initial guess. Our numerical results indicate that the CONVEX model gives almost the same restored images visually and numerically.

3.3. Comparison with other convex models. In this subsection, we compare the proposed model with other existing convex models [38] and [9]. The stopping criteria of the three numerical methods are measured on the relative change of the successive iterates to be less than a specified tolerance: $\|\mathbf{f}_k - \mathbf{f}_{k-1}\|_2 / \|\mathbf{f}_{k-1}\|_2 \leq 5 \times 10^{-4}$. The initial guess is set to be the observed image. We test the blurred and noisy images given in [9]. Here we set the values of μ based on (2.4) in the proposed model. The restored images by the proposed CONVEX model are given in Figures 15–18. The two parameters in Dong and Zeng's algorithm [9] are set the same as the default setting reported in [9]. The parameter α in Wang and Ng's algorithm [38] is set as the ℓ_1-norm of noise in the log-image domain, which was also used in [38]. The values of regularization parameters used by different methods are also shown in the captions of the figures. When we compare our restoration results with those of the convex model [9], the visual performance of the proposed CONVEX model is better than that of the convex model [9]. In Table 3, we also list the average of PSNR values, iterations, and computational time (in seconds) over ten noise cases under the same experimental setting (type of blur and level of noise). We see that the performance of the proposed CONVEX model is better than that of the convex model [9] and Wang and Ng's method [38] in terms of PSNR values, iterations, and computational time.

In Figures 19–22, we further give the restoration results when Rayleigh or Gaussian noise is used. We note that existing convex models [38] and [9] assume the Gamma noise to be added in the degradation process. Here we set the values of μ based on the formulas in (2.5) and (2.6) in the proposed model. The values of regularization parameters used by different methods are also shown in the captions of Figures 19–22. We see from the figures that the visual quality of the restored images is quite good.

(a) (b) (c) (d)

Figure 9. (a) *The observed image corrupted by motion blur and the Gamma noise, and the restored image by* (b) *the AA model using guess* 1 *(*$\alpha = 3 \times 10^{-1}$*),* (c) *the AA model using guess* 2 *(*$\alpha = 3 \times 10^{-1}$*), and* (d) *the CONVEX model (*$\alpha_2 = 9 \times 10^{-4}$*).*

(a) (b) (c) (d)

Figure 10. (a) *The observed image corrupted by Gaussian blur and the Gamma noise, and the restored image by* (b) *the AA model using guess* 1 *(*$\alpha = 3 \times 10^{-1}$*),* (c) *the AA model using guess* 2 *(*$\alpha = 3 \times 10^{-1}$*), and* (d) *the CONVEX model (*$\alpha_2 = 1 \times 10^{-3}$*).*

(a) (b) (c) (d)

Figure 11. (a) *The observed image corrupted by Moffat blur and the Gamma noise, and the restored image by* (b) *the AA model using guess* 1 *(*$\alpha = 3 \times 10^{-1}$*),* (c) *the AA model using guess* 2 *(*$\alpha = 3 \times 10^{-1}$*), and* (d) *the CONVEX model (*$\alpha_2 = 1.2 \times 10^{-3}$*).*

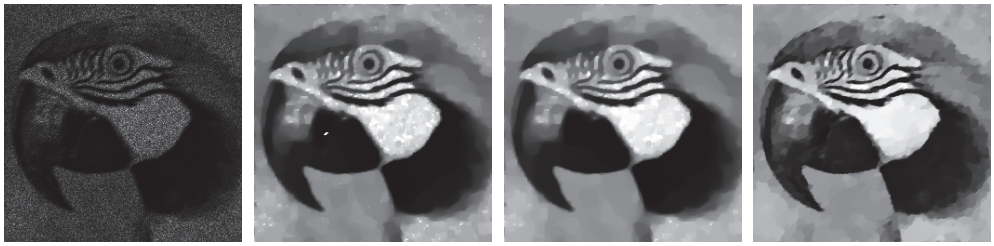

(a) (b) (c) (d)

Figure 12. (a) *The observed image corrupted by motion blur and the Gamma noise, and the restored image by* (b) *the AA model using guess* 1 *(*$\alpha = 3 \times 10^{-1}$*),* (c) *the AA model using guess* 2 *(*$\alpha = 3 \times 10^{-1}$*), and* (d) *the CONVEX model (*$\alpha_2 = 6 \times 10^{-4}$*).*

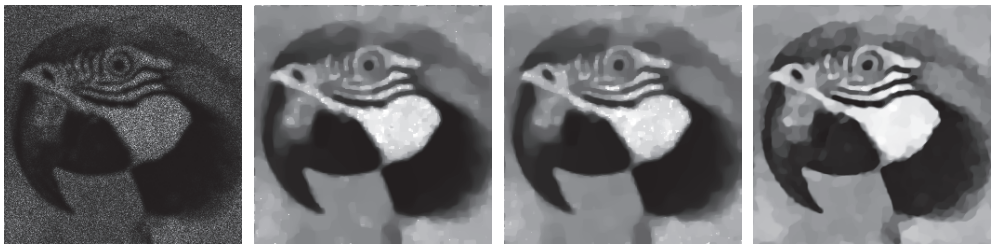

(a) (b) (c) (d)

Figure 13. (a) *The observed image corrupted by Gaussian blur and the Gamma noise, and the restored image by* (b) *the AA model using guess* 1 *(*$\alpha = 3 \times 10^{-1}$*),* (c) *the AA model using guess* 2 *(*$\alpha = 3 \times 10^{-1}$*), and* (d) *the CONVEX model (*$\alpha_2 = 4 \times 10^{-4}$*).*

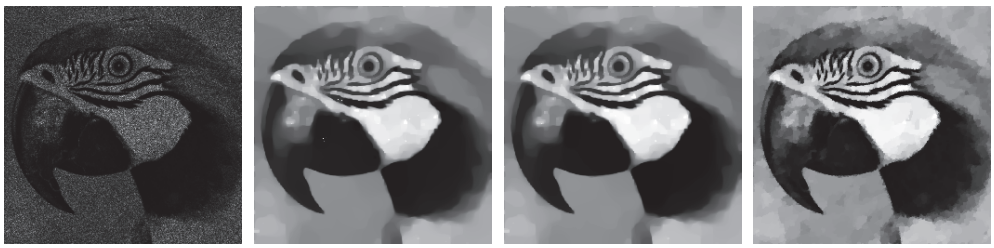

(a) (b) (c) (d)

Figure 14. (a) *The observed image corrupted by Moffat blur and the Gamma noise, and the restored image by* (b) *the AA model using guess* 1 *(*$\alpha = 4 \times 10^{-1}$*),* (c) *the AA model using guess* 2 *(*$\alpha = 4 \times 10^{-1}$*), and* (d) *the CONVEX model (*$\alpha_2 = 8 \times 10^{-4}$*).*

(a) (b) (c) (d)

Figure 15. (a) *The observed image corrupted by motion blur and Gamma noise,* (b) *the restored image by Wang and Ng's model* ($\alpha = 1.7 \times 10^4$), (c) *the restored image by Dong and Zeng's model* ($\lambda = 9 \times 10^{-2}$ *and* $\alpha = 1.6 \times 10^1$), *and* (d) *the restored image by the CONVEX model* ($\alpha_2 = 9 \times 10^{-4}$).

(a) (b) (c) (d)

Figure 16. (a) *The observed image corrupted by Gaussian blur and Gamma noise,* (b) *the restored image by Wang and Ng's model* ($\alpha = 1.7 \times 10^4$), (c) *the restored image by Dong and's Zeng model* ($\lambda = 7 \times 10^{-2}$ *and* $\alpha = 1.6 \times 10^1$), *and* (d) *the restored image by the CONVEX model* ($\alpha_2 = 1 \times 10^{-3}$).

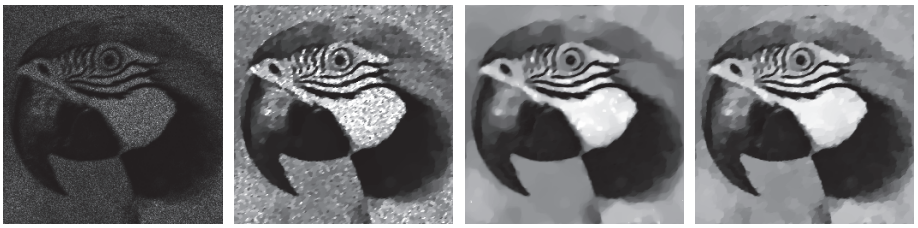

(a) (b) (c) (d)

Figure 17. (a) *The observed image corrupted by motion blur and Gamma noise,* (b) *the restored image by Wang and Ng's model* ($\alpha = 1.7 \times 10^4$), (c) *the restored image by Dong and Zeng's model* ($\lambda = 8 \times 10^{-2}$ *and* $\alpha = 1.6 \times 10^1$), *and* (d) *the restored image by the CONVEX model* ($\alpha_2 = 6 \times 10^{-4}$).

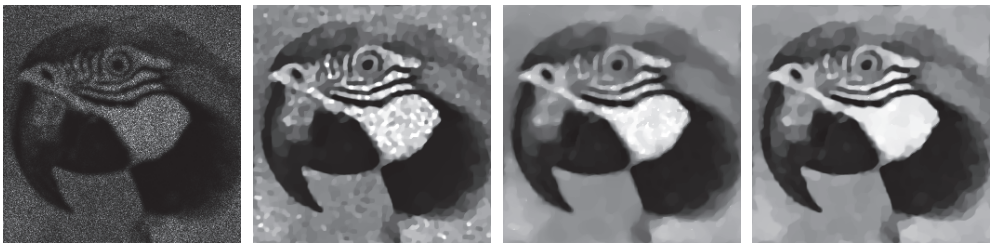

(a) (b) (c) (d)

Figure 18. (a) *The observed image corrupted by Gaussian blur and Gamma noise,* (b) *the restored image by Wang and Ng's model* ($\alpha = 1.7 \times 10^4$), (c) *the restored image by Dong and Zeng's model* ($\lambda = 7 \times 10^{-2}$ *and* $\alpha = 1.6 \times 10^1$), *and* (d) *the restored image by the CONVEX model* ($\alpha_2 = 4 \times 10^{-4}$).

Table 3

The comparison results of different models for multiplicative deblurring.

Images	Blurs	Wang and Ng's model			Dong and Zeng's model			CONVEX model		
		PSNR	Iter	Time	PSNR	Iter	Time	PSNR	Iter	Time
(a)	Motion	21.60	410.0	17.0	22.91	261.0	96.0	23.35	93.0	4.0
	Gaussian	21.48	620.0	26.0	21.98	293.0	93.0	22.42	35.0	2.0
(b)	Motion	20.80	460.0	20.0	23.04	300.0	199.0	23.18	106.0	5.0
	Gaussian	20.98	404.0	17.0	21.12	303.0	204.0	21.33	25.0	1.0

(a) (b) (c) (d)

Figure 19. (a) *The observed image corrupted by Motion blur and the Gaussian noise,* (b) *the restored image by the CONVEX model* ($\alpha_2 = 7 \times 10^{-4}$, *PSNR:* 24.18*dB, time:* 7.0*s*), (c) *the observed image corrupted by Motion blur and the Rayleigh noise, and* (d) *the restored image by the CONVEX model* ($\alpha_2 = 7 \times 10^{-3}$, *PSNR:* 20.78*dB, time:* 4.0*s*).

Figure 20. (a) *The observed image corrupted by Gaussian blur and the Gaussian noise,* (b) *the restored image by the CONVEX model* ($\alpha_2 = 7 \times 10^{-4}$, *PSNR:* 22.93*dB, time:* 2.0*s*), (c) *the observed image corrupted by Gaussian blur and the Rayleigh noise, and* (d) *the restored image by the CONVEX model* ($\alpha_2 = 6 \times 10^{-3}$, *PSNR:* 20.40*dB, time:* 4.0*s*).

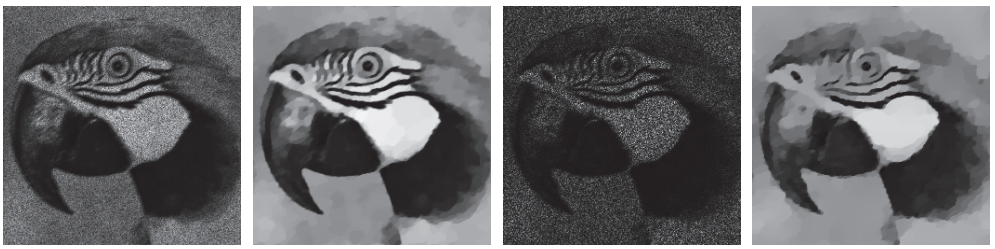

(a) (b) (c) (d)

Figure 21. (a) *The observed image corrupted by Motion blur and the Gaussian noise,* (b) *the restored image by the CONVEX model* ($\alpha_2 = 6 \times 10^{-4}$, *PSNR:* 24.61*dB, time:* 3.0*s*), (c) *the observed image corrupted by Motion blur and the Rayleigh noise, and* (d) *the restored image by the CONVEX model* ($\alpha_2 = 5 \times 10^{-3}$, *PSNR:* 19.99*dB, time:* 4.0*s*).

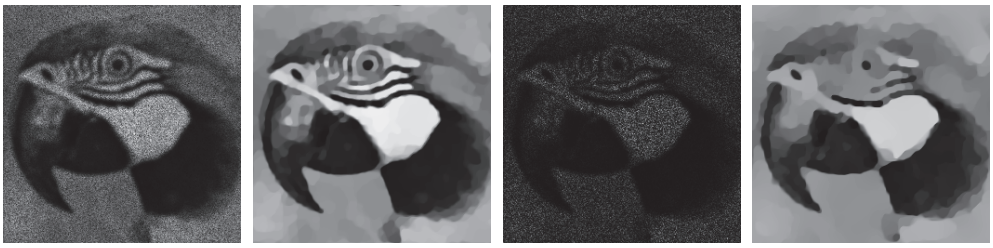

Figure 22. (a) *The observed image corrupted by Gaussian blur and the Gaussian noise,* (b) *the restored image by the CONVEX model* ($\alpha_2 = 5 \times 10^{-4}$, *PSNR:* 22.30*dB, time:* 3.0*s*), (c) *the observed image corrupted by Gaussian blur and the Rayleigh noise, and* (d) *the restored image by the CONVEX model* ($\alpha_2 = 5 \times 10^{-3}$, *PSNR:* 18.89*dB, time:* 5.0*s*).

3.4. Estimation of μ. In section 2, we have discussed how to estimate the mean value of $\mathbf{w}$ theoretically (Gamma and Rayleigh noises) and numerically (Gaussian noise). In this subsection, we study the effect of μ experimentally for image restoration results. We use the actual generated noise $\mathbf{n}$ in the examples of section 3.1 to estimate the mean value $\bar{w}$ of $\mathbf{w}$ from the noise realization. We test different values of μ as follows: $\bar{w} - 0.2$, $\bar{w} - 0.15$, $\bar{w} - 0.1$, $\bar{w} - 0.05$, $\bar{w}$, $\bar{w} + 0.05$, $\bar{w} + 0.1$, $\bar{w} + 0.15$, $\bar{w} + 0.2$. The corresponding restoration results in PSNR are given in Table 4. As for the comparison, the last column gives the PSNR values of the restored images when the values of μ are used based on the formulas in (2.4), (2.5), and (2.6) in the proposed model. We note that the PSNR values of the restored images are almost the same when the values calculated from the formulas or $\bar{w}$ are used. It is natural to note that when the input value of μ is far from the estimated mean value of $\mathbf{w}$, the PSNR values of the restored images decrease.

Table 4
The restoration results for different values of estimated μ.

Images	Noise	Estimated values									μ
		-0.2	-0.15	-0.1	-0.05	0	0.05	0.1	0.15	0.2	
Cameraman	Gaussian	19.22	21.34	23.81	26.20	26.86	25.02	22.51	20.24	18.32	26.86
	Gamma	20.33	22.33	24.24	25.19	24.39	22.61	20.61	18.80	17.22	24.42
	Rayleigh	18.63	19.70	20.71	21.52	21.94	21.81	21.18	20.22	19.12	21.94
Parrot	Gaussian	19.34	21.39	23.79	26.23	27.21	25.74	23.29	21.15	19.41	27.26
	Gamma	20.47	22.41	24.27	25.31	24.75	23.10	21.30	19.70	18.30	24.76
	Rayleigh	18.62	19.50	20.24	20.71	20.74	20.46	19.79	18.85	17.97	20.77

4. Concluding remarks. In this work, we have proposed an unconditional convex variational model for recovering blurred images corrupted by multiplicative noise of different types. In the model, we studied the functional by minimizing two variables: the restored image and the noise image on the ℓ_1 data-fitting term, the variance term, and the TV regularization term. We developed an efficient alternating direction method for solving the proposed model. Extensive numerical experiments are provided to illustrate the state-of-the-art performance of the proposed model.

5. Acknowledgments. We would like to thank the authors of [9], Yi-Qiu Dong and Tie-Yong Zeng, for providing their code and original images, and the referees for providing valuable comments and insightful suggestions which have improved to several aspects of this manuscript.

REFERENCES

[1] S. Aja-Fernández, G. Vegas-Sánchez-Ferrero, M. Martín-Fernández, and C. Alberola-López, *Automatic noise estimation in images using local statistics. Additive and multiplicative cases*, Image Vision Comput., 27 (2009), pp. 756–770.

[2] G. Aubert and J.-F. Aujol, *A variational approach to removing multiplicative noise*, SIAM J. Appl. Math., 68 (2008), pp. 925–946.

[3] J. M. Bioucas-Dias and M. A. Figueiredo, *Multiplicative noise removal using variable splitting and constrained optimization*, IEEE Trans. Image Process., 19 (2010), pp. 1720–1730.

[4] S. Boyd, N. Parikh, E. Chu, B. Peleato, and J. Eckstein, *Distributed optimization and statistical learning via the alternating direction method of multipliers*, Found. Trends Mach. Learn., 3 (2011), pp. 1–122.

[5] A. Chambolle and T. Pock, *A first-order primal-dual algorithm for convex problems with applications to imaging*, J. Math. Imaging Vision, 3 (2011), pp. 120–145.

[6] P. L. Combettes and J.-C. Pesquet, *Proximal splitting methods in signal processing*, in Fixed-Point Algorithms for Inverse Problems in Science and Engineering, Springer, New York, 2011, pp. 185–212.

[7] P. L. Combettes and R. W. Valarie, *Signal recovery by proximal forward-backward splitting*, Multiscale Model. Simul., 4 (2005), pp. 1168–1200.

[8] C. Deledalle, L. Denis, and F. Tupin, *Iterative weighted maximum likelihood denoising with probabilistic patch-based weights*, IEEE Trans. Image Process., 18 (2009), pp. 2661–2672.

[9] Y. Dong and T. Zeng, *A convex variational model for restoring blurred images with multiplicative noise*, SIAM J. Imaging Sci., 6 (2013), pp. 1598–1625.

[10] S. Durand, J. Fadili, and M. Nikolova, *Multiplicative noise removal using L1 fidelity on frame coefficients*, J. Math. Imaging Vision, 36 (2010), pp. 201–226.

[11] E. Esser, X. Zhang, and T. F. Chan, *A general framework for a class of first order primal-dual algorithms for convex optimization in imaging science*, SIAM J. Imaging Sci., 3 (2010), pp. 1015–1046.

[12] D. Evans, *Estimating the variance of multiplicative noise*, in Proceedings of the 18th International Conference on Noise and Fluctuations, AIP Conf. Proc. 780, AIP, Melville, NY, 2005, pp. 99–102.

[13] A. Fan, *A Variational Approach to MR Bias Correction*, Master's thesis, Massachusetts Institute of Technology, Cambridge, MA, 2003.

[14] D. Gabay and B. Mercier, *A dual algorithm for the solution of nonlinear variational problems via finite element approximation*, Comput. Math. Appl., 2 (1976), pp. 17–40.

[15] T. Goldstein and S. Osher, *The split Bregman method for L1-regularized problems*, SIAM J. Imaging Sci., 2 (2009), pp. 323–343.

[16] P. C. Hansen, J. G. Nagy, and D. P. O'leary, *Deblurring Images: Matrices, Spectra, and Filtering*, SIAM, Philadelphia, 2006.

[17] B. He and X. Yuan, *On the $O(1/n)$ convergence rate of the Douglas–Rachford alternating direction method*, SIAM J. Numer. Anal., 50 (2012), pp. 700–709.

[18] Y. Huang, L. Moisan, M. Ng, and T. Zeng, *Multiplicative noise removal via a learned dictionary*, IEEE Trans. Image Process., 21 (2012), pp. 4534–4543.

[19] Y. Huang, M. Ng, and T. Zeng, *The convex relaxation method on deconvolution model with multiplicative noise*, Commun. Comput. Phys., 13 (2013), pp. 1066–1092.

[20] Y.-M. Huang, M. K. Ng, and Y.-W. Wen, *A new total variation method for multiplicative noise removal*, SIAM J. Imaging Sci., 2 (2009), pp. 20–40.

[21] K. Krishnamoorthy, *Handbook of Statistical Distributions with Applications*, Chapman & Hall/CRC, Taylor & Francis Group, Boca Raton, FL, 2010.

[22] F. Li, M. K. Ng, and C. Shen, *Multiplicative noise removal with spatially varying regularization parameters*, SIAM J. Imaging Sci., 3 (2010), pp. 1–20.
[23] A. Montillo, J. K. Udupa, L. Axel, and D. N. Metaxas, *Interaction between noise suppression and inhomogeneity correction in MRI*, in Proceedings of SPIE, Vol. 5032, 2003, pp. 1025–1036.
[24] M. K. Ng, R. H. Chan, and W.-C. Tang, *A fast algorithm for deblurring models with Neumann boundary conditions*, SIAM J. Sci. Comput., 21 (1999), pp. 851–866.
[25] M. K. Ng, P. Weiss, and X. Yuan, *Solving constrained total-variation image restoration and reconstruction problems via alternating direction methods*, SIAM J. Sci. Comput., 32 (2010), pp. 2710–2736.
[26] M. Paul and T. Brandt, *Classification Methods for Remotely Sensed Data*, Taylor & Francis, New York, 2001.
[27] G. Ramponi, R. D'Alvise, and C. Moloney, *Automatic estimation of the noise variance in SAR images for use in speckle filtering*, in Proceedings of the IEEE-EURASIP Workshop on Nonlinear Signal and Image Processing (NSIP), 1999, pp. 835–838.
[28] L. Rudin, P.-L. Lions, and S. Osher, *Multiplicative denoising and deblurring: Theory and algorithms*, in Geometric Level Set Methods in Imaging, Vision, and Graphics, Springer, New York, 2003, pp. 103–119.
[29] L. Rudin, S. Osher, and E. Fatemi, *Nonlinear total variation based noise removal algorithms*, Phys. D, 60 (1992), pp. 259–268.
[30] L. F. Shampine, *Vectorized adaptive quadrature in MATLAB*, J. Comput. Appl. Math., 211 (2008), pp. 131–140.
[31] J. Shi and S. Osher, *A nonlinear inverse scale space method for a convex multiplicative noise model*, SIAM J. Imaging Sci., 1 (2008), pp. 294–321.
[32] G. Steidl and T. Teuber, *Removing multiplicative noise by Douglas-Rachford splitting methods*, J. Math. Imaging Vision, 36 (2010), pp. 168–184.
[33] A. Tekalp and G. Pavlovic, *Restoration of scanned photographic images*, in Digital Image Restoration, A. Katsaggelos, ed., Springer-Verlag, Berlin, 1991, pp. 209–239.
[34] T. Teuber and A. Lang, *Nonlocal filters for removing multiplicative noise*, in Scale Space and Variational Methods in Computer Vision, Springer, Berlin, Heidelberg, 2012, pp. 50–61.
[35] T. Teuber, G. Steidl, and R. H. Chan, *Minimization and parameter estimation for seminorm regularization models with I-divergence constraints*, Inverse Problems, 29 (2013), 035007.
[36] M. Tur, C. Chin, and J. Goodman, *When is speckle noise multiplicative?*, Appl. Opt., 21 (1982), pp. 1157–1159.
[37] R. F. Wagner, S. W. Smith, J. M. Sandrik, and H. Lopez, *Statistics of speckle in ultrasound B-scans*, IEEE Trans. Sonics Ultrason., 30 (1983), pp. 156–163.
[38] F. Wang and M. Ng, *A fast minimization method for blur and multiplicative noise removal*, Int. J. Comput. Math., 90 (2013), pp. 48–61.
[39] D. Yin, Y. Gu, and P. Xue, *Speckle-constrained variational methods for image restoration in optical coherence tomography*, J. Opt. Soc. Amer., 30 (2013), pp. 878–885.
[40] S. Yun and H. Woo, *A new multiplicative denoising variational model based on mth root transformation*, IEEE Trans. Image Process., 21 (2012), pp. 2523–2533.